Ionospheric-Scale Index Map Based on TEC Data for South America

Clezio M. Denardini, Giorgio A. S. Picanço, Paulo F. Barbosa Neto, Paulo A. B. Nogueira, Carolina S. Carmo, Laysa C. A. Resende, Juliano Moro, Sony S. Chen, Esmeralda Romero-Hernandez, Regia P. Silva, and Cristiano M. Wrasse

Abstract – This article gives a summary of our comprehensive study for developing an ionospheric-scale index map based on the Disturbance Ionospheric Index (DIX). This index aims to target all the different user groups affected by ionospheric disturbances—navigation, positioning, and satellite-communication users—in a simple and straightforward approach. Therefore, we used the vertical total electron content (TEC) over South America to calculate the TEC maps covering latitudes from 60°S to 20°N and longitudes from 90°W to 30°W, with 0.5° × 0.5° resolution. Afterward, DIX maps were obtained to reveal the variation of the TEC over an average quiet ionosphere background. In order to illustrate the use of the index map, the ionospheric disturbances after and during the 2015 Saint Patrick's Day magnetic storm are presented as an example of the disturbances in the DIX at different latitudinal ranges.

Manuscript received 29 April 2020.

C. M. D. thanks CNPq/MCTI (303643/2017-0). G. A. S. P. thanks Capes/MEC (88887.467444/2019-00). P. F. B. N. thanks Capes/MEC (1622967). C. S. C. thanks CNPq/MCTI (88887.479226/2020-00). S. S. C. thanks CNPq/MCTI (134151/2017-8) and Capes/MEC (88887.362982/2019-00). L. C. A. R. thanks NSSC/CAS. J. M. thanks NSSC/CAS and the CNPq/MCTI (429517/2018-01). R. P. S. thanks CNPq/MCTI (300986/2020-3).

C. M. Denardini, G. A. S. Picanço, C. S. Carmo, S. S. Chen, R. P. Silva, and C. M. Wrasse are with the National Institute for Space Research, São José dos Campos, São Paulo 12227-010, Brazil; e-mail: clezio.denardin@inpe.br, giorgio.picanco@inpe.br, carolina.carmo@inpe.br, sony.chen@inpe.br, regia.pereira@inpe.br, cristiano.wrasse@inpe.br.

P. F. Barbosa Neto is with the National Institute for Space Research, São José dos Campos, São Paulo 12227-010, Brazil; and Salesian University Center of São Paulo, Lorena, São Paulo 12600-100, Brazil; e-mail: paulo.barbosa@inpe.br.

P. A. B. Nogueira is with the Federal Institute of Education, Science and Technology of São Paulo, Jacareí, São Paulo 12322-030, Brazil; e-mail: paulo.nogueira@ifsp.edu.br.

L. C. A. Resende is with the National Institute for Space Research, São José dos Campos, São Paulo 12227-010, Brazil; and the State Key Laboratory of Space Weather, National Space Science Center, Chinese Academy of Science, Beijing, China; e-mail: laysa.resende@inpe.br.

J. Moro is with the State Key Laboratory of Space Weather, National Space Science Center, Chinese Academy of Science, Beijing, China; and the Southern Regional Space Research Center, Santa Maria, Rio Grande do Sul, Brazil; e-mail: juliano.moro@inpe.br.

E. Romero-Hernandez is with Universidad Autónoma de Nuevo León, Facultad de Ciencias Físico-Matemáticas, LANCE, Monterrey, Mexico; e-mail: cefeyda_esm@yahoo.com.mx.

1. Introduction

Space weather effects on the Earth and near-Earth assets have become of great interest in the last decade, motivating studies on economic impacts (e.g., [1]) and risk assessment (e.g., [2]). As a result, several economic sectors that depend on space weather conditions (as defined by [3]) are driving a growing demand for global indices to represent the impact of the solar-terrestrial interaction (external effects of space weather) as well as the "extreme" variation of the near-Earth environment (internal effects of space weather). In this last category is the Earth's ionosphere, whose condition/state is quite complicated to forecast, depending on both the solar wind and magnetosphere forcing [4] and the local electrodynamic effects [5]. For example, in studying the ionospheric impact on communication, [6] states that energy that fuels the variability of the ionosphere may ultimately derive from the sun. However, that study highlights that secondary energy sources from below the ionosphere (e.g., atmospheric gravity waves) may also contribute to developing ionospheric irregularities.

In such a scenario of a complex ionosphere driven by external and internal forcing, it seems reasonable to make an effort to develop an index as a proxy (in a more or less specific way) of complex ionospheric behavior to improve customer decisions. In addition, regional differences (e.g., latitude, longitude, daytime/nighttime, declination, presence of anomalies) may in turn require local indices for dealing with the regional effects. This is especially true over South America, where [7] recently provided evidence of the joint effect of the equatorial ionization anomaly (EIA) and South America Magnetic Anomaly for irregularities which are scintillation-effective.

Indeed, several indices have been developed over the decades to represent ionospheric conditions, and comparative studies have been published. In [8], the responses were compared of some of these indices to ionospheric phenomena such as the presence of large-scale gradients, and scintillation revealed that they may respond differently to different phenomena. Also, a single comparison of the S4 to the rate of TEC index (ROTI) revealed a day-to-day variability [9] of this ratio, varying from circumstances when those two indices correlate well to when they do not correlate [10]. Such results were interpreted in [11] in terms of a latitudinal dependence of the ROTI. Recently, [12] stated that the "anisotropy of field-aligned irregularities in the low-latitude ionosphere has a very significant

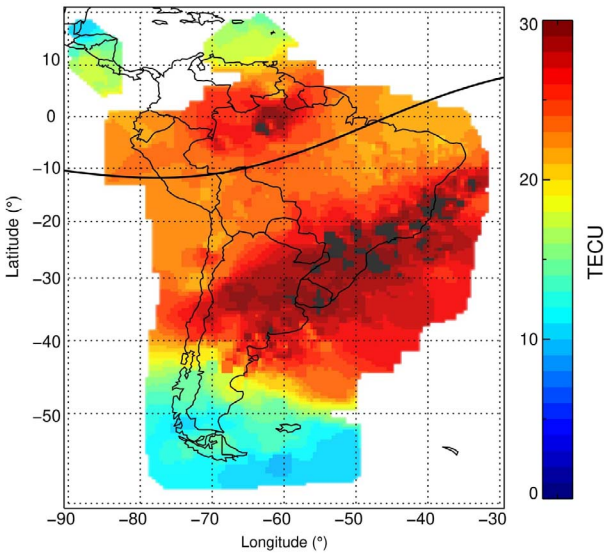

Figure 1. Embrace/INPE Space Weather TEC Map at 18:30 UT on 14 February 2017.

impact on the characteristics of the scintillations observed," which is measured by the S4 index.

In [13], a new ionospheric disturbance index was proposed, named DIX (Disturbance Ionosphere indeX), which is an alternative to the dichotomy of S4 versus ROTI. A recent study on this index [14] claimed that this time series index can better characterize temporal and spatial ionospheric variations on small to medium scales, and stated that the existing indices available for space weather still inadequately address the ionospheric effects of the solar-terrestrial interaction.

In this work, we show that the DIX is an appropriate index to represent ionospheric disturbances, but there is some room for improvement. Also, as it was conceived, its representation of ionospheric disturbances seems to be limited mainly to external drivers. Nevertheless, it is well known that the ionosphere responds to both external drivers (e.g., [15, 16]) and internal ones [17]. Moreover, internal drivers do not necessarily occur during magnetically disturbed periods. Indeed, the most dramatic phenomena of the ionosphere (e.g., equatorial plasma bubbles) are regularly observed along the magnetic equator all over the globe (e.g., [18, 19]) during magnetically quiet times.

Therefore, we performed studies aiming to extend the DIX representation of ionospheric variability to cover the ionospheric response to both external and internal drivers. The whole development of this new approach for calculating the DIX is detailed in [20], where some comparison with the original DIX may also be found. In the present work, we summarize those studies to support our decision to use the new equation presented going forward. Nevertheless, our results already point out that regional ionospheric indices are more suitable for properly describing ionospheric effects due to space weather events. Also, their area of coverage should reflect (but not be limited to) localized effects, such as lower latitudinal effects versus higher latitudinal ones, daytime versus nighttime, and magnetic anomalies.

2. Methodology

We used the TEC map [21] developed at the Brazilian Studies and Monitoring of Space Weather program (Embrace/INPE) as input, which is a customization of the earlier procedure by [22]. An example of the Embrace/INPE Space Weather TEC Map is presented in Figure 1, which provides the TEC obtained for the period between 18:20 and 18:30 UT on 14 February 2017 with individual cells of 0.5° × 0.5° resolution over the whole of South America, corresponding to a 60 km^2 × 60 km^2 grid.

Note that the measurements are not homogeneously distributed all over the map, which may lead to over- and underrepresented areas where the number of receivers was more and less densely distributed. Also, there may be some interpolation where no data were available. The solid black line across the map provides the location of the magnetic equator in 2017.

The DIX for a cell (or observation point) can be calculated from (1), which we have evolved from [13] to contribute to this significant initial step:

$$\mathrm{DIX}_k(t) = \left| \frac{\alpha\left(\Delta\mathrm{TEC}_k(t) \Big/ \Delta\mathrm{TEC}_k^{\mathrm{Qd}}(t)\right) + \Delta\mathrm{TEC}_k(t)}{\beta} \right| \tag{1}$$

A detailed description of the terms and coefficients of this equation is presented in [23] and therefore will not be presented in detail here, nor the reasons why and how they were established. Nevertheless, we mention that $\mathrm{TEC}_k(t)$ is the TEC provided by the TEC map procedure for cell k, $\mathrm{TEC}_k^{\mathrm{Qd}}(t)$ represents the "average" behavior of the TEC at a given time over the observation point, and $\Delta\mathrm{TEC}_k(t) = \mathrm{TEC}_k(t) - \mathrm{TEC}_k^{\mathrm{Qd}}(t)$ is the difference between the current TEC and the undisturbed TEC for cell k. The coefficient α is the $\mathrm{TEC}_k^{\mathrm{Qd}}(t)$ at midnight, which consequently is obtained for each period of analysis, and is used to combine a term that gives the difference between the current TEC and the undisturbed TEC with a term that provides the ratio of the variation and aims to identify fluctuation in the TEC. The coefficient β is a latitude-dependent factor used to normalize the DIX output into a scale that ranges from 0 to 5. It may range from 5 to 50 TEC units at a specific location. Figure 2 illustrates an example of the time variation of the DIX as calculated in the present work (red curve) along with the DIX as calculated with the original equation (blue area). The *Kp* values are plotted in the upper portion of the graph so the reader can have an idea of the response of both versions of DIX in response to their fluctuation.

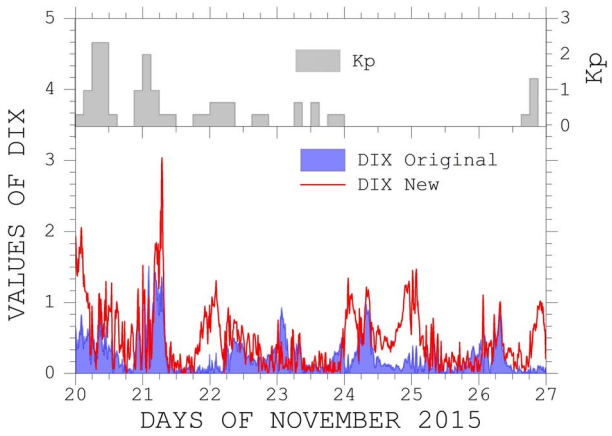

Figure 2. Example of the time variation of the DIX as calculated in the present work (red), the DIX as calculated originally (blue), and the *Kp* index (gray).

3. Results and Discussions

In order to exemplify the result, we selected the period around the Saint Patrick's Day magnetic storm, 16 to 19 March 2015. The Storm Sudden Commencement (SSC) for this magnetic storm occurred at 04:45 UT on 17 March and was caused by a halo-type coronal mass ejection reaching the Earth's magnetosphere, associated with a C9-class flare (at 02:13 UT) coming from Active Region 2297. The values of the Dst index floated close to zero during the days before the storm and reached –223 nT at 23:00 UT; the recovery phase lasted until around 12:00 UT on 22 March, when the Dst recovered to 10% of its lowest value.

A set of DIX maps is presented in Figure 3, covering the part of the period described in the foregoing, calculated with the original method (upper six maps) and the current method (bottom six maps). Although the time resolution between DIX maps is 10 minutes, we present one map every 12 h only, due to the limited extent of this publication. When compared, the corresponding maps look similar. But the higher DIX values are revealed by our method, like the result shown for quiet time presented in Figure 2.

On 16 March 2015 (Figure 3), prior to the geomagnetic storm, we identify a few high-DIX patches at low latitudes but not at the equator. We also observe DIX patches at low latitudes at 00:00 UT. These patches are similar to those high-TEC "islands" identified over northern Europe by [13]. In that case, they were attributed to convection of plasma from the North American region, and to severe amplitude and phase scintillations observed in coincidence with steep TEC gradients (characteristic of the edge of polar cap patches). We do not have a complete explanation yet for this observation. However, our analysis over São José dos Campos, Brazil, for the Saint Patrick's Day storm indicates that the event was characterized by a wavelike oscillation in the TEC (not shown here) that started to grow with respect to the average daily behavior of the TEC at 00:00 UT (21:00 LT) until about 02:30 UT (23:30 LT), then decreased until 03:30 UT (00:30 LT). Then it rose again until before 05:00 UT (02:00 LT), then declined to match the average daily behavior at 06:30 UT (03:30 LT). Thus, it might be that a traveling ionospheric disturbance or a neutral atmosphere wave interaction acted to organize the plasma up to develop localized plasma instabilities. In any case, such a localized signature on the DIX without any magnetic disturbance is an indication that the index reacts to internal drivers.

Afterward, as observed during the storm, the DIX patches reduced in intensity while moving around the low-latitude region or even completely vanished. The intensity of the DIX in the patches was clearly reinforced again. The ionospheric disturbance reappeared several hours after the SSC of the Saint Patrick's Day magnetic storm. The DIX reached level 4 (mainly correlated with the southern crest of the EIA) a few hours after the maximum effect in the ring current was reached, i.e., the lowest Dst value was registered.

For the present case, this high DIX value was observed at 21:00 LT (00:00 LT on 18 March 2015), when no fountain effect was any longer playing a role at the equator (see [24, fig. 1]). This pattern persisted over the next hours, when the DIX map showed level 5 all over the crests of the EIA for the storm. Consequently, we conclude by highlighting two main features of these new DIX maps: the response is localized geographically (not global) and includes the manifestation of internal drivers in the ionosphere.

4. Conclusions

We have developed a disturbance ionospheric index, based on previous studies, to investigate the deviation of ionospheric content from its background pattern based on GNSS TEC data collected over the whole of South America. We have advanced the analysis of the index by including ΔTEC variations to better represent the deviations of the GNSS TEC from its normal behavior. By including the coefficient α along with selecting the average behavior of the TEC in the DIX equation, we are able to show variation observed in the ionosphere that cannot be attributed to external drivers. Furthermore, we introduce the coefficient β, based on the study of the latitudinal impact of geomagnetic storms over the ionosphere in South America, to define "extreme" for each latitudinal range and standardize the excursion of DIX between 0 and 5, with 5 being the highest level of ionospheric disturbance. After this modification, a general analysis of the DIX response to the Saint Patrick's Day magnetic storm revealed two main features of the new DIX: its response is localized geographically (not global) and includes the manifestation of internal drivers in the ionospheric variability. Finally, the collected data used in the present study are fully open and accessible at the Embrace Program website (http://www.inpe.br/spaceweather).

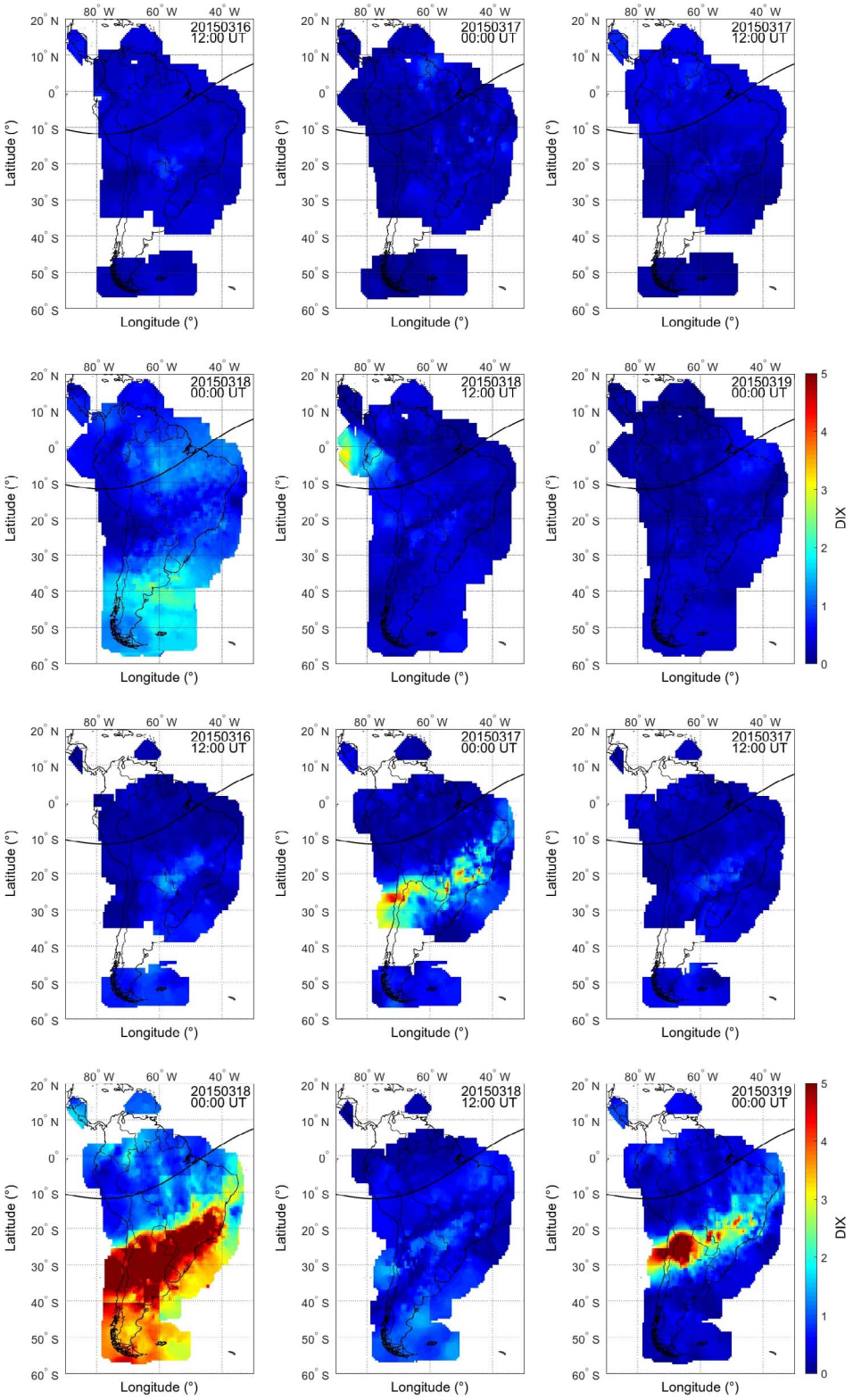

Figure 3. Sequence of DIX maps obtained from 12:00 UT on 16 March 2015 to 00:00 UT on 19 March 2015 (with 12 h resolution), around the Saint Patrick's Day magnetic storm, using (upper six maps) the original method and (lower six maps) the current method.

5. Acknowledgments

The authors thank the Embrace/INPE Space Weather Program for providing the TEC maps, the Instituto Brasileiro de Geografia e Estatística for providing the raw TEC data, and the Divisão de Aeronomia (INPE) for providing the ionosonde data to Embrace/INPE. The data used in the present study are fully open and accessible at the Embrace Program (http://www.inpe.br/spaceweather).

6. References

1. J. P. Eastwood, E. Biffis, M. A. Hapgood, L. Green, M. M. Bisi, et al., "The Economic Impact of Space Weather: Where Do We Stand?," *Risk Analysis*, **37**, 2, February 2017, pp. 206-218.
2. J. C. Green, J. Likar, and Y. Shprits, "Impact of Space Weather on the Satellite Industry," *Space Weather*, **15**, 6, June 2017, pp. 804-818.
3. C. M. Denardini, S. Dasso, and J. A. Gonzalez-Esparza, "Review on Space Weather in Latin America. 3. Development of Space Weather Forecasting Centers," *Advances in Space Research*, **58**, 10, November 2016, pp. 1960-1967.
4. Y. Wei, B. Zhao, G. Li, and W. Wan, "Electric Field Penetration Into Earth's Ionosphere: A Brief Review for 2000–2013," *Science Bulletin*, **60**, 8, April 2015, pp. 748-761.
5. K. Venkatesh, P. R. Fagundes, D. S. V. V. D. Prasad, C. M. Denardini, A. J. De Abreu, et al., "Day-to-Day Variability of Equatorial Electrojet and Its Role on the Day-to-Day Characteristics of the Equatorial Ionization Anomaly over the Indian and Brazilian Sectors," *Journal of Geophysical Research: Space Physics*, **120**, 10, October 2015, pp. 9117-9131.
6. J. M. Goodman, "Operational Communication Systems and Relationships to the Ionosphere and Space Weather," *Advances in Space Research*, **36**, 12, 2005, pp. 2241-2252.
7. L. Spogli, L. Alfonsi, V. Romano, G. De Franceschi, G. M. Joao Francisco, et al., "Assessing the GNSS Scintillation Climate Over Brazil Under Increasing Solar Activity," *Journal of Atmospheric and Solar-Terrestrial Physics*, **105–106**, December 2013, pp. 199-206.
8. A. Bhattacharyya, T. L. Beach, S. Basu, and P. M. Kintner, "Nighttime Equatorial Ionosphere: GPS Scintillations and Differential Carrier Phase Fluctuations," *Radio Science*, **35**, 1, January–February 2000, pp. 209-224.
9. S. Basu, K. Groves, J. Quinn, and P. Doherty, "A Comparison of TEC Fluctuations and Scintillations at Ascension Island," *Journal of Atmospheric and Solar-Terrestrial Physics*, **61**, 16, November 1999, pp. 1219-1226.
10. T. L. Beach and P. M. Kintner, "Simultaneous Global Positioning System Observations of Equatorial Scintillations and Total Electron Content Fluctuations," *Journal of Geophysical Research: Space Physics*, **104**, A10, October 1999, pp. 22553-22565.
11. K. S. Jacobsen, "The Impact of Different Sampling Rates and Calculation Time Intervals on ROTI Values," *Journal of Space Weather and Space Climate*, **4**, 2014, p. A33.
12. C. S. Carrano, K. M. Groves, and C. L. Rino, "On the Relationship Between the Rate of Change of Total Electron Content Index (ROTI), Irregularity Strength (C_kL), and the Scintillation Index (S_4)," *Journal of Geophysical Research: Space Physics*, **124**, 3, March 2019, pp. 2099-2112.
13. N. Jakowski, C. Borries, and V. Wilken, "Introducing a Disturbance Ionosphere Index," *Radio Science*, **47**, 4, August 2012, p. RS0L14.
14. V. Wilken, M. Kriegel, N. Jakowski, and J. Berdermann, "An Ionospheric Index Suitable for Estimating the Degree of Ionospheric Perturbations," *Journal of Space Weather and Space Climate*, **8**, 2018, p. A19.
15. A. D. Richmond, C. Peymirat, and R. G. Roble, "Long-Lasting Disturbances in the Equatorial Ionospheric Electric Field Simulated With a Coupled Magnetosphere-Ionosphere-Thermosphere Model," *Journal of Geophysical Research: Space Physics*, **108**, A3, March 2003, pp. 1118-1130.
16. R. P. Silva, J. R. Souza, J. H. A. Sobral, C. M. Denardini, G. L. Borba, et al., "Ionospheric Plasma Bubble Zonal Drift Derived From Total Electron Content Measurements," *Radio Science*, **54**, 7, 2019, pp. 580-589.
17. M. A. Abdu, "Equatorial Spread F and Ionosphere-Thermosphere System: A Review," *Geophysical Research Letters*, **2**, 1993, pp. 193-209.
18. F. D. Chu, J. Y. Liu, H. Takahashi, J. H. A. Sobral, M. J. Taylor, et al., "The Climatology of Ionospheric Plasma Bubbles and Irregularities Over Brazil," *Annales Geophysicae*, **23**, 2, 2005, pp. 379-384.
19. T. Farges and P. M. Vila, "Equatorial Spread and Dynamics in the F Layer Over West Africa From Ionogram Analysis, During the Declining Solar Flux Year 1994–1995," *Journal of Atmospheric and Solar-Terrestrial Physics*, **65**, 14–15, September–October 2003, pp. 1309-1314.
20. G. A. S. Picanço, *Development and Analysis of an Ionospheric Index Based on Data From Total Electron Content*, master's thesis, National Institute for Space Research–INPE, São José dos Campos, Brazil, 2019.
21. H. Takahashi, C. M. Wrasse, C. M. Denardini, M. B. Pádua, E. R. de Paula, et al., "Ionospheric TEC Weather Map Over South America," *Space Weather*, **14**, 11, November 2016, pp. 937-949.
22. Y. Otsuka, T. Ogawa, A. Saito, T. Tsugawa, S. Fukao, et al., "A New Technique for Mapping of Total Electron Content Using GPS Network in Japan," *Earth, Planets and Space*, **54**, 1, 2002, pp. 63-70.
23. C. M. Denardini, G. A. S. Picanço, P. F. Barbosa Neto, P. A. B. Nogueira, C. S. Carmo, et al., "Ionospheric Scale Index Map Based on TEC Data for Space Weather Studies and Applications," *Space Weather*, **18**, 9, 2020, pp. e2019SW002328.
24. B. G. Fejer, E. R. de Paula, S. A. Gonzalez, and R. F. Woodman, "Average Vertical and Zonal F Region Plasma Drifts Over Jicamarca," *Journal of Geophysical Research: Space Physics*, **96**, A8, August 1991, pp. 13901-13906.